CdS Covered with Ga-P Electron Exchange Membrane for Efficient Photocatalytic Hydrogen Prodection

Zejin Wang, Linqing Zhang and Zhiliang Jin*

School of Chemistry and Chemical Engineering, Key Laboratory for Chemical Engineering and Technology, State Ethnic Affairs Commission, North Minzu University, Yinchuan 750021, PR China

Abstract: CdS is one of the best semiconductor photocatalysts. However, photocorrosion will occur when CdS takes part in the photocatalytic system. The general solution is to add sacrificial reagents to inhibit this phenomenon. Even so, it can not maintain the stability of CdS. In order to improve the stability and efficiency of CdS in pure water, Ga-P electron exchange membrane was designed to modify its surface. Under radiation of visible light, a significant increase can be observed in hydrogen production activity. In the absence of Pt as electron transfer agent, the modification of Ga-P realizes decomposition of pure water from zero to one. At the same time, the hydrogen production rate is increased about 5 times with Pt and catalytic life is greatly extended. Through proof of controlled experiment, Ga-P electron exchange membrane can not only prolong the lifetime of photogenerated electrons, but also change the direction of electrons. The formation of a protective membrane makes composite photocatalyst improve the stability and enhance the photocatalytic activity. Based on the analysis of TEM, fluorescence lifetime, UV-Vis diffuse reflection and photocurrent response, the mechanism is analyzed from atomic radius, nuclear orbit and energy level. For homogeneous electronic band structure and XPS analysis, we determined that the binary catalyst formed an S-scheme heterojunction. The work provides a potential way to design a more efficient and stable composite photocatalyst in the future. And contributed to the development of S-scheme heterojunctions.

Keywords: Photocorrosion, Ga-P electron exchange membrane, Visible light, Decomposition of pure water, Catalytic life.

1. INTRODUCTION

The massive use of fossil fuel has caused ever-worsening environmental problems. It is urgent to effectively develop technologies for obtaining clean energy [1]. Semiconductor photocatalysis technology emerges as the times require [2]. Ideally, water will be directly resolved into hydrogen and oxygen under the condition of photocatalyst under the irradiation of sunlight [3]. However, the seemingly simple process is not so easy to achieve. Therefore, the selection of highly efficient and stable photocatalysts has become the primary condition in the field of research. For example, TiO_2 and CdS have always been the focus of research [4]. But there has been no substantial progress because of different shortcomings. Due to its wide bandgap, TiO_2 can only use the ultraviolet band which is 5% of the total solar radiation. The efficiency can not be greatly improved. Some related studies have used semiconductor doping to form intermediate energy levels to enhance the absorption range of TiO_2. but the doped part is still unstable in pure water [5]. CdS is an ideal photocatalytic material because of its 2.3 eV bandgap and thermodynamic requirement of water splitting. However, photoetching near anions caused by photogenerated holes reduces its stability [6]. In order to solve these problems, electron sacrificial agents are often added to the reaction system to consume photogenerated holes, thus increasing the lifetime of photogenerated electrons and inhibiting photoinduced corrosion. But this method consumes sacrificial reagents, more like sacrificial reagents, and catalysts react with water instead of directly using solar photocatalysis to decompose water [7]. Hydrogen precipitation is at the expense of electronic sacrificial agents. Therefore, we start with CdS to improve its photocatalytic performance and stability in pure water.

To solve the photocorrosion of CdS without sacrificing reagents providing electrons for holes, the idea is to coat the surface of CdS with a layer of membrane that allowed electrons to selectively penetrate [8]. Because of the formation of CdS, S and Cd shared electron pair. In order to achieve the protection function of the membrane, it is required to select more stable membrane material with more share electrons but could not hinder the reaction [9]. Considering the radius of cluster atoms, it required to select the atoms with smaller size and smaller relative atomic mass as the coating. The difference between size and mass could form another power source of electron exchange under the action of gravity. After careful consideration, the element gallium and phosphorus were chosed to be membrane material. The electronic arrangement of was $4s^2 4p^1$, which was

*Address correspondence to this author at the School of Chemistry and Chemical Engineering, Key Laboratory for Chemical Engineering and Technology, State Ethnic Affairs Commission, North Minzu University, Yinchuan 750021, PR China; E-mail: zl-jin@nun.edu.cn

E-ISSN: 2410-2199/23

located in the group IIIA and the fourth period. Ga often showed as +3 in its compounds and P just matched it. The combination of these two elements might lead to form more stable protective membrane, which could serve as a bridge for electronic exchange [10].

In this work, CdS nanorods was synthesized by a simple hydrothermal method [11]. Next, Ga-P was coated on the surface of CdS nanorods for inhibit photocorrosion and form an S-scheme heterojunction to promote hydrogen production. Under the condition of adding Pt as electron transfer agent on the surface of composite photocatalyst, the electrons of CdS were excited by visible-light energy and transferred from valence band to conduction band. After passing through the Ga-P electron exchange membrane (EEM), they contacted with water by the active site of Pt. This process could reduce H^+ in water to H_2 [12]. The electrons of the remaining oxidized radicals also return to the holes in CdS through the Ga-P EEM. Sacrificial reagents were not suitable for the whole process and the system showed a good stability. Through controlled experiment and characterization analysis, we gave out a deeper understanding of the internal mechanism. It provided a reference for improving the life of photocatalyst.

2. EXPERIMENTAL SECTION

2.1. Sample Preparation Procedure

All chemicals were Analytical Reagent and Chemically Pure without further purification. Cadmium nitrate tetrahydrate ($CdN_2O_6{\cdot}4H_2O$, Tianjin Kermel Chemical Reagent Co., Ltd, AR, ≥99.0%), Thiourea (CH_4N_2S, Tianjin Fengyue Chemical Co., Ltd, AR, ≥99.0%), Gallium nitrate ($Ga(NO_3)_3{\cdot}xH_2O$, BEIJING HUAGONGCHANG, CP, ≥99.0%), Red Phosphorus, (P, BEIJING HONGXINGHUAGONGCHANG, AR, ≥99.0%), Ethylenediamine ($H_2NCH_2CH_2NH_2$, Xilong Scientific Chemical Co., Ltd., AR, ≥99.0%), Potassium Chloroplatinate (K_2PtCl_6, SHENYANG KEDASHIJICHANG Co., Ltd, AR, ≥99.0%), Sodium sulfate (Na_2SO_4, Xilong Scientific Co., Ltd., AR, > 99%) were used as provided.

2.1.1. Preparation of CdS Nanorod

CdS nanorod was prepared by traditional hydrothermal synthesis [13]. $CdN_2O_6{\cdot}4H_2O$ (3.86 g) and CH_4N_2S (2.85 g) were dissolved in 50 mL ethylenediamine solution. After stirring for 15 min, the mixed solution was transferred into a 100 mL PTFE (Polytetrafluoroethylene) lining of reaction caldron. Then, the reactor was placed in oven at 160 °C for 24 h. The product needed to be separated by centrifuge and washed with acetone,ethanol and deionized water. After washing, the CdS nanorod was put into oven at 80 °C for drying for 10 h.

2.1.2. Synthesis of Ga-P@CdS

CdS, P and $Ga(NO_3)_3{\cdot}xH_2O$ were put into a mortar and ground evenly. The ratio of material dosage was shown in Table **1**. The grinding uniform powder was added to the ethylenediamine solution. After stirring evenly, the solution was put in the reactor which was also placed in oven at 160°C for 12 h. Similarly, the product was washed and dried according to the above washing method. Finally, all the photocatalysts were grinded and collected.

2.1.2. Synthesis of Pt/Ga-P@CdS

Pt was deposited on the surface of composite photocatalyst by photodeposition [14]. The specific steps are as follows: Ga-P@CdS photocatalyst (50 mg) was added into 150 mL quartz reaction bottle. After adding 90 mL of water, the bottle was placed into the ultrasonic machine until the photocatalyst was evenly dispersed in the water. 200 μL of K_2PtCl_6 solution (2.5 g/L) was dropped in the bottle. And Pt was deposited on the Ga-P@CdS photocatalyst after the condition of stirring and illumination for 1 h.

2.2. Characterization

The photocatalyst samples were characterized by means of transmission electron microscopy (Tecnai-

Table 1: Composition of Composite Photocatalysts with Different Proportions

Sample Material	CdS Nanorod (g)	$Ga(NO_3)_3{\cdot}xH_2O$ (g)	P (g)
Ga-P@CdS-1	0.2	0.5	0.02
Ga-P@CdS-2	0.2	0.5	0.04
Ga-P@CdS-3	0.2	0.5	0.06
Ga-P@CdS-4	0.2	0.5	0.08

G2-F30) field emission transmission electron microscope operating at accelerating voltage of 300 kV for the morphologies and microstructures. The spectrum of chemical composition and elemental state were collected on VG Scientific ESCALAB 250Xi-XPS photoelectron spectrometer with an Al Kα X-ray resource. Fluorescence spectra was characterized by FluoroMAX-4 spectrometer (HORIBA Scientific, France) at room temperature. X-ray diffraction (XRD) was recorded on a Rigaku B/Max-RB X-ray diffractometer with a nickel-filtrated Cu Kα radiation in the 2θ ranging from 10 to 80°. The UV-Vis DRS of the catalyst was performed on a UV-2550 (Shimadzu) spectrometer which $BaSO_4$ powder was used as the internal standard to obtain the optical properties of the samples. The photoelectrochemical experiments were carried out on a Princeton electrochemical workstation (PAR Versa STAT 4). The saturated calomel electrode (SCE) and the Pt electrode were worked as the reference electrode and the counter electrode. The prepared photocatalysts were adhered to working electrode on the surface of the FTO through Nation solution. In order to simulate electron transfer in a photocatalytic reaction system, the electrolyte was made of 0.2 mol/L Na_2SO_4 solution. The soaking area of the working electrode was controlled in 1 cm^2. A 300-W Xe lamp with cut-off filter(λ ≥ 420 nm) was used as light source. Photocurrent-time curves was tested under open circuit voltage. LSV was tested from -0.6 V to 0 V. The electrochemical impedance spectroscopy (PEIS) was fitted by ZSimDemo [15-17].

2.3. Photocatalytic Hydrogen Evolution Experiments

The hydrogen evolution experiment was taken in quartz reaction bottle (180 mL). The rated power of the irradiation source was 300 W, which was simulated sunlight (λ≥ 420 nm). The illumination area was 5 cm^2. In experiment, 50 mg photocatalyst and 120 mL deionized water were added and evenly stirred. The air in the quartz reactor was replaced by argon. Extract 0.5 mL of gas from bottle each hour. Gas generated by the reaction was detected by gas chromatography (Agilent 6820, TCD, 13× columns, Ar carrier). The hydrogen content was calculated by standard curve [18]. The apparent quantum efficiency (AQE) was measured under the 300 W Xe lamps. The light source was changed by using different fillets of 430, 460, 490, 520 and 550 nm. Photon flflux of the incident light was determined using a Ray virtual radiation actinometer (FU 100, silicon ray detector, light spectrum, 400~700 nm; sensitivity, 10–50 $\mu V \mu mol^{-1} m^{-2} s^{-1}$). The AQE was measured through the equation below (1) [19, 20]:

$$AQE(\%) = \frac{number\ of\ reacted\ electrons}{number\ of\ incident\ photons} \times 100\% = \frac{number\ of\ evolved\ H_2\ molecules \times 2}{number\ of\ incident\ photons} \times 100\% \quad (1)$$

3. RESULTS AND DISCUSSION

3.1. Structure and Composition of Photocatalysts

TEM was used to observe the morphology and structure of the composite photocatalyst. As shown in Figure **1**, different multiples TEM images of Ga-P@CdS composite photocatalyst with different multiples were listed. It can be seen from the low power electron micrograph in Figure **1A** that the composite photocatalyst was uniformly distributed in the form of nanorod with some stacking. With the increase of electron microscope power in Figure **1B**, the membrane of Ga-P became more and more obvious, just like pocky. Furthermore, the change of lattice fringes can be observed by HRTEM. Due to the poor crystallinity of Ga-P films and the analysis of GaP as an amorphous material in the above XRD characterization, GaP does not have lattice fringes similar to fingerprints and is irregularly distributed. However, the lattice fringe of CdS nanorods was clear. SAED image can only observe the star distribution map of CdS, The SAED image can only observe the stellar distribution map of CdS, which also proves that GaP is an amorphous catalyst. So for further observation, the element mapping was added to show the distribution of various elements. As shown in the Figure **1E**, the area in the yellow box was selected for area scanning. The results were shown in the right figures that elements of Ga and P were wrapped around Cd and S. It can be seen that, as mentioned above, CdS nanorod was indeed wrapped by Ga-P EEM [21-23].

In order to further confirm crystal structure of the photocatalyst, XRD test was carried out for analysis. The following Figure **2** showed the X-ray diffraction of the photocatalyst components. It can be clearly seen that pure CdS nanorods had better crystalline state, which corresponded well with PDF#41-1049. The diffraction peaks correspond to the crystal planes of CdS, respectively. Meanwhile, it can be clearly seen that the intensity of the diffraction peak of CdS decreased obviously when CdS was covered by Ga-P. It can also be proved that amorphous Ga-P membrane was coated on the surface of CdS. Meanwhile, it can be clearly seen that the intensity of the diffraction peak of CdS decreased obviously when CdS was covered by

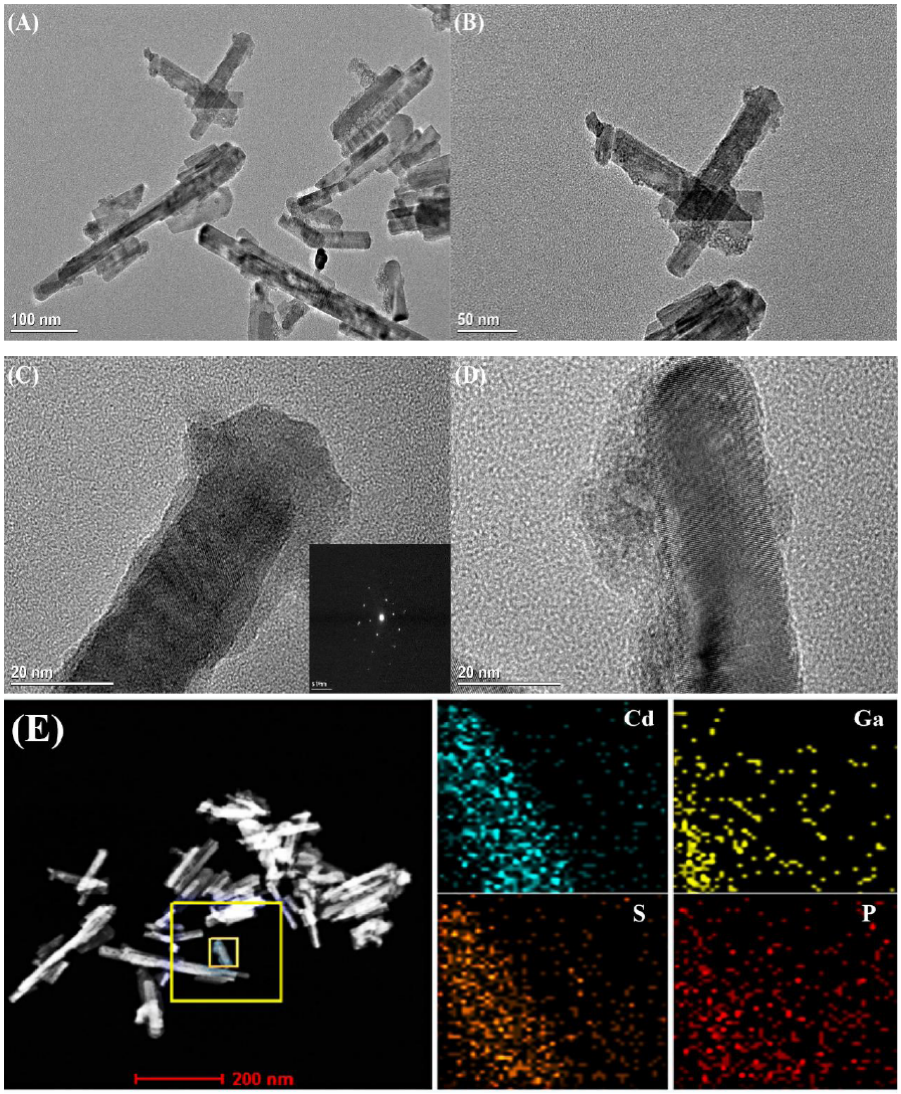

Figure 1: TEM images (**A**) (**B**), HRTEM images (**C**) (**D**) and element mapping (**E**) of Ga-P@CdS.

Ga-P. It can also be proved that amorphous Ga-P membrane was coated on the surface of CdS [24-26].

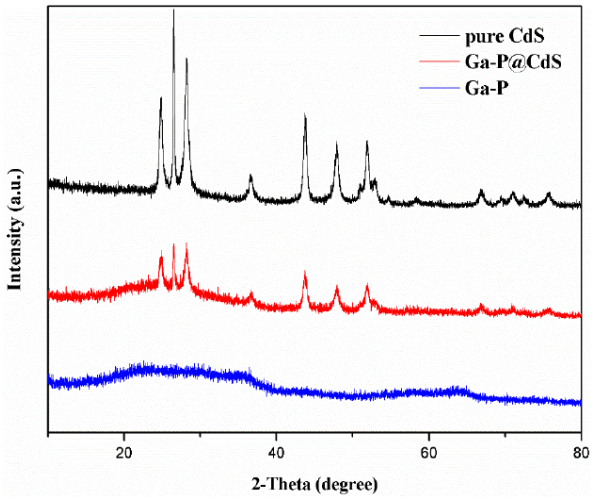

Figure 2: XRD pattern of CdS, Ga-P, Ga-P@CdS.

XPS was used to further investigate the chemical composition and elemental state of the internal elements of the composite photocatalyst. The results of XPS in Figure **3** were analyzed in depth, especially the Ga-P membrane. As can be seen from Figure **3A** and **3D**, CdS was definitely synthesized. In Figure **3C**, there were signal peaks with the binding energy of large spacing in Ga. It illustrated that there were two different gallium compounds in the Ga-P EEM. Compared with energy spectrum of P 2p, Ga-P electron exchange membrane mainly contained both GaP and $GaPO_4$. GaP, as a semiconductor with a band gap of 2.2 eV, can exchange electrons with CdS by forming heterojunction. According to the previous literature, we can also observe that the Binding energy of Cd and S in CdS moves in the direction where the Binding energy is effective, and the Binding energy of Ga and P in GaP moves in the direction where the Binding

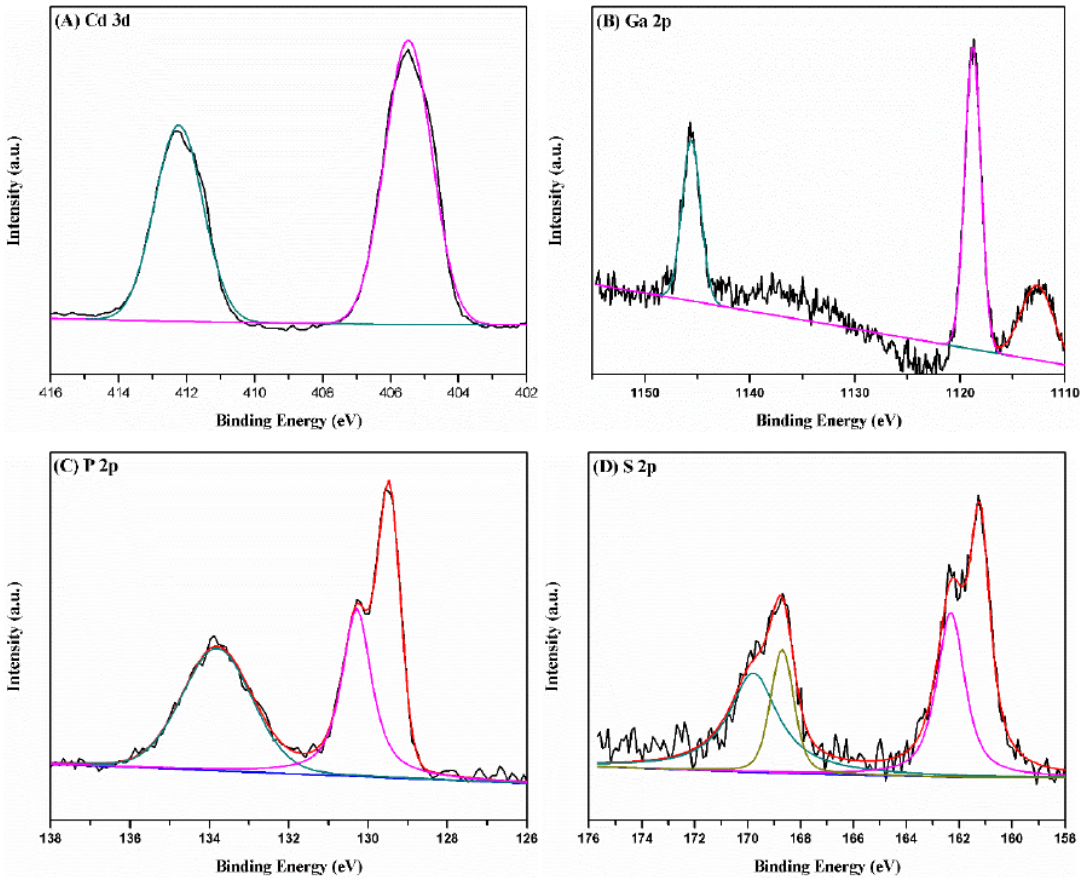

Figure 3: XPS spectra of Ga-P@CdS sample: (**A**) Cd 3d, (**B**)Ga 2p, (**C**) P 2p, (**D**) S 2p.

energy is reduced. Furthermore, as a transparent and stable insoluble phosphate, $GaPO_4$ provided protection for the whole photocatalyst system and prevented the photocatalyst from contacting strong oxidized free radical. Only when they combined together can improve the efficiency of electronic transmission and inhibit the effect of light corrosion [27-29]. We also used XPS valence band spectroscopy to analyze the valence band positions of various elemental catalysts, and the results will be presented in the mechanism.

3.2. Optical Properties of Photocatalysts

Then the optical properties of the composite photocatalyst were tested. It can be seen from Figure **4A** of UV-Vis DRS that the absorption edge of the pure phase CdS was 520 nm. But the absorbance of composite photocatalysts were improved after 520 nm when the surface of CdS nanorods was covered with Ga-P electron exchange membrane. It proved that the coating of Ga-P membrane did not weaken the

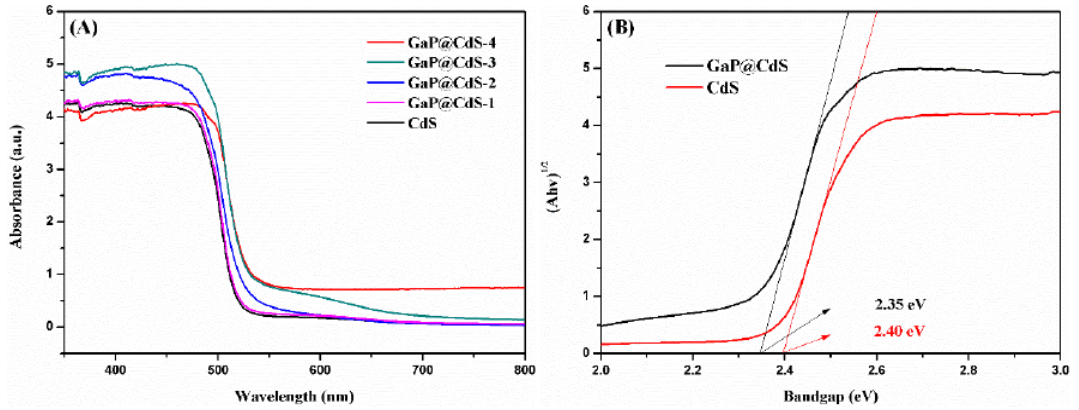

Figure 4: The UV–vis absorption spectra (**A**) and the width of bandgap of CdS, Ga-P@CdS (**B**).

absorption range of CdS. And with the increase of Ga-P content, the increase of absorption was more obvious. At the same time, band-gap of photocatalyst was calculated and compared in Figure **4B** by the Tauc plot method (2). It can be seen that the band-gap was shortened from 2.40 eV to 2.35 eV after coverd with Ga-P EES. The shortening of the band-gap indicated that the transition of electrons from valence band to conduction band became easier under exposure to visible light. This was helpful to enhance the reaction activity of photocatalyst in water [30-32].

$$(\alpha hv)^{1/n} = A(hv - E_g) \quad (2)$$

Where α is absorbance, h is Planck constant, v is frequency, A is constant and Eg is bandgap width.

Hydrogen production activity test was the most intuitive explanation for photocatalyst activity test. Under 420 nm visible light, the activity of the Ga-P@CdS composite photocatalyst in pure water was shown in the Figure **5**. Figure **5A** showed the comparison between CdS and Ga-P@CdS. It can be seen that CdS cannot generate hydrogen in pure water. But the activity of Ga-P@CdS composite photocatalyst increased significantly when CdS was covered with Ga-P EEM. At the same time, At the same time, Pt particles were added to photocatalysts as electron transfer sites by photoreduction. After adding Pt particles, as shown in Figure **B**, CdS can decompose water and had strong activity. However, it can be seen that its photocatalytic activity can only be maintained for 20 h. This was due to the influence of light corrosion, which led to the denaturation of the outer photocatalyst and stopped the reaction. While the photocatalytic rate of the Ga-P@CdS did not decrease significantly in 50 h under the protection of Ga-P EEM. At the same time, the cycle stability test was also carried out. The catalyst was tested in a 5-hour cycle. The gas in the reaction vessel was replaced with Ar after each cycle. The results was shown in Figure **5C**. There was no change of activity rate in 25 h, which proved the photocatalyst was stable. Due to the low amount of oxygen produced, it was speculated that the reason was dissolved oxygen or free radical combined oxygen in water to corrode the photocatalyst. Therefore, 2 mL PFDL was added to the reaction system for adsorbing O_2. It can be seen in Figure **5d** that the hydrogen production activity of the composite

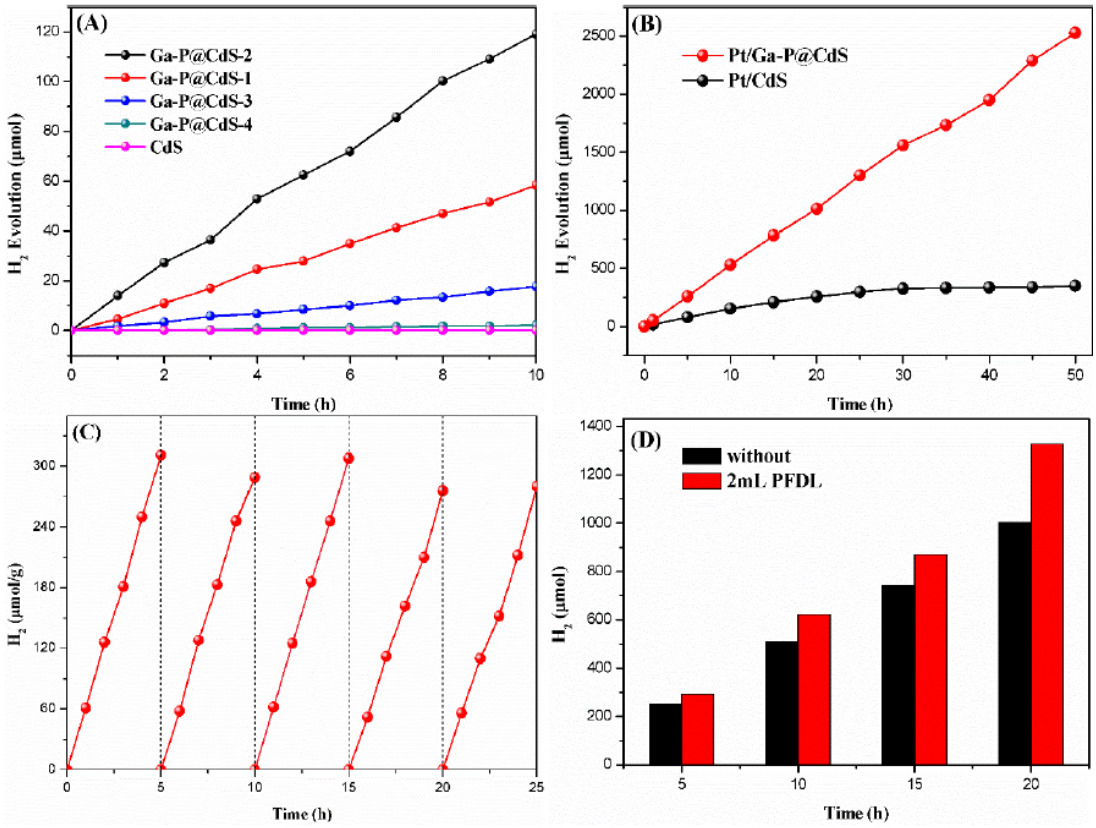

Figure 5: Hydrogen production trend of the photocatalysts (**A**), hydrogen production of photocatalysts with Pt (**B**), cycle stability test of Pt/Ga-P@CdS (**C**) and hydrogen production after adding 2 mL PFDL in the reaction system.

photocatalyst was significantly improved. It not only showed that the reaction went forward after removing dissolved oxygen, but also proved that the composite photocatalyst can decompose water [33-35].

Finally, the AQE of the composite photocatalyst was measured under different wavelengths. It can be seen in Figure **6** that the highest AQE was 0.18% at 430 nm. As the wavelength of the light source became longer, the AQE became lower and lower. It was because the longer the wavelength of light, the smaller the energy it can provide [36].

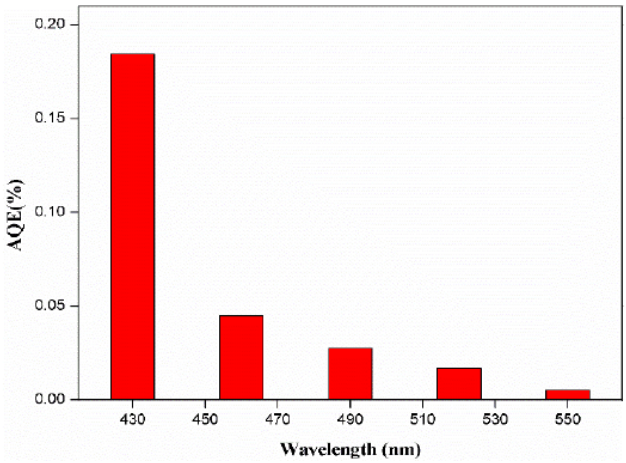

Figure 6: The AQE of Pt/Ga-P@CdS composite photocatalyst at different wavelengths.

In order to further explore the Promoting effect of Ga-P EEM on CdS, time-resolved PL measurements were exhibited. As a function of time, the TRPL are fit using a dbl-exponential decay model using the following Equation (3) [37].

As shown in Figure **7**, the time-resolved photoluminescence (TRPL) spectra of Ga-P@CdS exhibited a slower PL decay compared with CdS. It revealed that Ga-P@CdS can keep the charges separation for long time. In addition, we investigated steady-state fluorescence, with the composite binary photocatalyst having the lowest fluorescence intensity and the lowest recombination efficiency. The fitting parameters were given in Table **5**. Table **5** listed the lifetime of photocatalysts and pointed out their percentage. To better evaluate the influence of Ga-P on CdS emission decay, we calculate the average lifetimes according to Equation (4) [38].

Compared with the CdS, the average lifetime of Ga-P@CdS was increased to 1.92 ns. These results indicated that Ga-P EEM on the surface of CdS provided a path for photogenerated charge transfer. Thus PL lifetime was increased and photogenerated charge was separated effectively, thereby photocatalytic activity was enhanced [39].

$$I(t) = \sum_{i=1,2,3} B_i \exp(-t/\hat{\alpha}) \quad (3)$$

Where I is normalised emission intensity, τ_i is respectively decay lifetime of luminescence; B_i is the corresponding weight factors.

$$<\hat{o}> = \sum_{i=1,2,3} B_i \hat{o}_i^2 / \sum_{i=1,2,3} B_i \hat{\alpha} \quad (4)$$

Where <τ> is the average lifetime, τ_i is respectively decay time of the individual components; B_i is the corresponding weight factors.

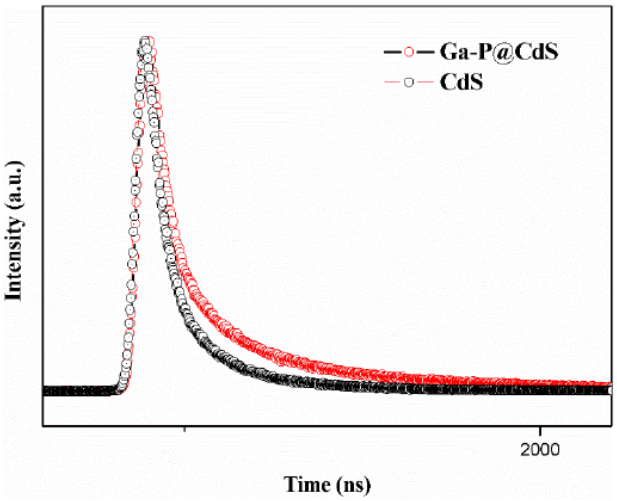

Figure 7: Time-resolved photoluminescence (TRPL) spectra of CdS and Ga-P@CdS.

Table 2: Kinetic Analysis of Emission Decay

Parameters / Samples	A_1 (%)	τ_1 (ns)	A_2 (%)	τ_2 (ns)	A_3 (%)	T_3 (ns)	<τ> (ns)	χ^2
CdS	44.29	1.85	30.37	0.30	25.34	6.67	0.76	1.32
Ga-P@CdS	33.65	3.47	28.09	0.71	38.26	13.83	1.92	1.06

3.3. The Electrochemical Characterization Test of Photocatalysts

In order to further explore the role of the Ga-P EEM, the photoelectrochemical performance of the photocatalyst were tested in 0.2 mol/L Na_2SO_4 solution. Figure **8A** showed comparison of photocurrent-time curves between pure CdS and composite photocatalysts with different content of Ga-P EEM. It was easy to observe that the photocurrent response of the composite photocatalysts would be greatly affected when the content of Ga-P EEM changed. The optical response of FTO/Ga-P@CdS-1 electrode was the strongest, but photo corrosion happened obviously. This causes the photocurrent to gradually decrease accordingly. It was because the formation of $GaPO_4$ in Ga-P EEM was not enough to play a protective role. FTO/ Ga-P@CdS-2 the photocurrent response is the most stable and photocurrent was as strong as FTO/Ga-P@CdS-1 after 250 s. However, if there were too many $GaPO_4$ in Ga-P EEM, the electron transfer would be hindered. It was reflected in the decrease of photocurrent, which was even lower than that of pure CdS. The results further illustrated that Ga-P EEM with appropriate element ratio can effectively transfer electrons and inhibit photocorrosion [40, 41].

The same thing happened in Electrochemical impedance spectroscopy (EIS). EIS test was an effective method to reflect the resistance of charge transfer in catalyst electrode. Figure **8B** showed EIS Nyquist plots of CdS, Ga-P@CdS-1, Ga-P@CdS-2 and Ga-P@CdS-4. It was well known that the radius of curvature in the EIS Nyquist plots corresponded to the impedance of the electrode. The larger the curvature radius of the curve, the greater the resistance of the catalyst, which also leads to a greater resistance to electron transfer. The results also correspond to the photocurrent results analyzed above, not that a larger proportion is better. Only a suitable proportion of catalysts can effectively improve the performance of composite catalysts. Ga-P@CdS-1 The smallest curvature radius indicates that it has the smallest resistance, and it also indirectly indicates that the GaP protective film can wrap around the surface of CdS, effectively suppressing its photo corrosion. [42]. We also carried out Motto characterization of the catalyst, and the results were explained by our electronic band structure in the hydrogen production mechanism.

3.4. Reaction Mechanism of Photocatalyst

The mechanism of the entire photocatalytic reaction process is shown in Figure **9**. Upon careful observation, it can be observed that two catalysts form an S-scheme heterojunction. When the two catalysts first come into contact, they undergo band bending, and ultimately CdS and GaP reach an equilibrium state. Under visible light irradiation, electrons in the valence band of CdS are excited and transferred to the conduction band. Then, when transferred to the valence band of GaP, the holes in the valence band of GaP are consumed, so that more Electron transfer are transferred to the conduction band. A large part of the electrons combine with H^+ at the Pt site, and a small part of the electrons produce hydrogen at the GAPS quilting cotton. At the same time as the reaction proceeds, due to the absence of electrons, the holes on CdS have the attraction of capturing electrons in water through Ga-P EEM. This is the entire process of electron acquisition and loss. The electron changes in Ga-P EEM are shown in the enlarged section of Figure **9**. The GaP in Ga-P EEM is used to receive and transfer transition electrons from CdS. Due to its

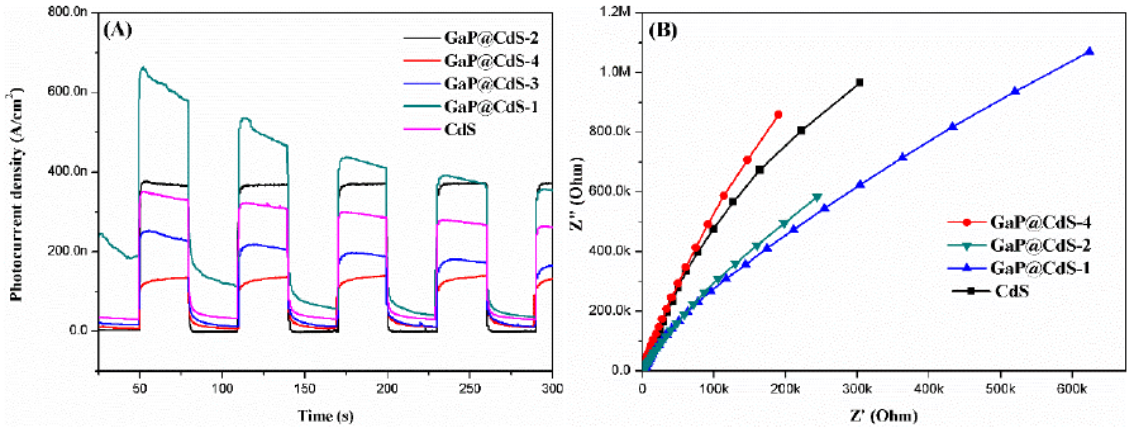

Figure 8: Photocurrent response of photocatalysts (**A**) and electrochemical impedance spectroscopy (**B**) pattern.

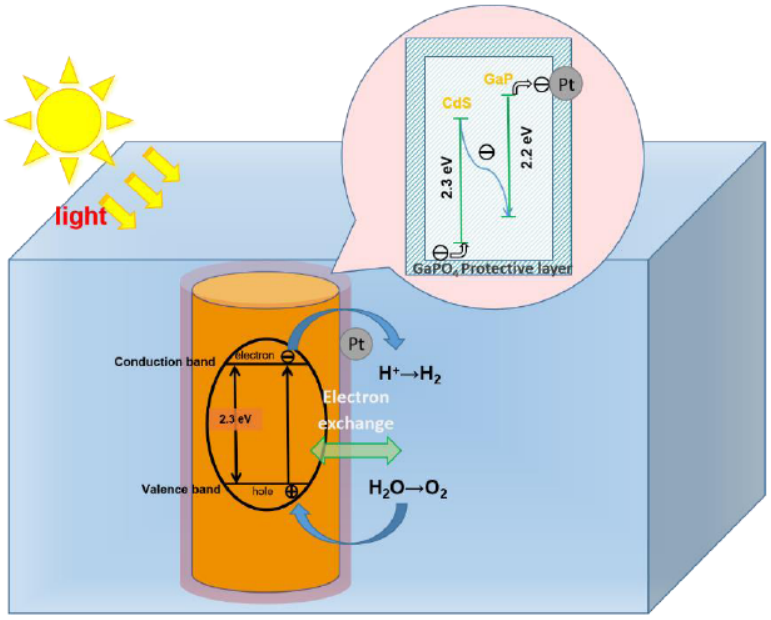

Figure 9: Reaction mechanism of photocatalyst of Pt/Ga-P@CdS composite photocatalyst.

semiconductor properties, it can form heterojunction structures with CdS. When CdS wants to capture electrons, $GaPO_4$ in Ga-P EEM separates strong oxidizing radicals from the surface of the photocatalyst to achieve overall stability. Therefore, the electron recycling in the whole system is always stable under the protection of Ga-P EEM [43].

CONCLUSION

In brief, we designed and successfully synthesized Ga-P@CdS composite photocatalyst. In the performance test, the Ga-P@CdS composite photocatalyst can effectively decompose water. Through various characterizations, we have proved the existence of Ga-P EEM and verified its performance. The CdS nanorods covered with Ga-P EEM can be seen clearly under HRTEM. The AQE of composite photocatalyst in pure water can reach 0.18% and it can keep stable under cyclic test and long time irradiation. All the results showed that it had the effect of accelerating electron exchange and inhibiting light corrosion. Finally, we vividly described the reaction mechanism in the whole system. These works not only provided a reference for improving the efficiency of photocatalyst, but also provided an effective method for enhancing the stability of photocatalyst.

AUTHOR CONTRIBUTIONS

Zejin Wang and Zhiliang Jin conceived and designed the experiments; Zejin Wang, performed the experiments; Zhiliang Jin contributed reagents/materials and analysis tools; Zejin Wang and Linqing Zhang wrote the paper.

CONFLICTS OF INTEREST

The authors declare that they have no competing interests.

REFERENCE

[1] Yang Liu, Xuqiang Hao, Haiqiang Hu, Zhiliang Jin. High efficiency electron transfer realized over NiS2/MoSe2 S-scheme heterojunction in photocatalytic hydrogen evolution, Acta Physico-Chimica. Sinica., 2021, 37(6), 2008030. https://doi.org/10.3866/PKU.WHXB202008030

[2] Dujuan Li, Xiaoli Ma, Peng Su, Shengjiang Yang, Zhibo Jiang, Youji Li, Zhiliang Jin, Effect of phosphating on NiAl-LDH layered double hydroxide form S-scheme heterojunction for photocatalytic hydrogen evolution, Molecular Catalysis, 2021, 516, 111990. https://doi.org/10.1016/j.mcat.2021.111990

[3] Teng Yan, Xiaojie Zhang, Hua Liu, Zhiliang Jin, CeO2 particles anchored to Ni2P nanoplate for efficient photocatalytic hydrogen evolution, Chinese Journal of Structural Chemistry, 2022, 41, 2201047-2201053.

[4] Dandan Liu, Haiou Liang, Chunping Li, Jie Bai, CdS nanoparticles with highly exposed (1 1 1) facets decorated on Pt/TiO2 nanotubes for highly efficient photocatalytic H2 evolution. Applied Surface Science, 2022, 586, 152711. https://doi.org/10.1016/j.apsusc.2022.152711

[5] Lijun Zhang, Xuqiang Hao, Junke Li, Yuanpeng Wang, Zhiliang Jin, Unique synergistic effects of ZIF-9(Co)-derived cobalt phosphide and CeVO4 heterojunction for efficient hydrogen evolution, Chinese Journal of Catalysis, 2020, 41, 82 - 94. https://doi.org/10.1016/S1872-2067(19)63454-6

[6] Guorong Wang, Yongkang Quan, Kaicheng Yang, Zhiliang Jin, EDA-assisted synthesis of multifunctional snowflake-Cu2S/CdZnS S-Scheme heterjunction for improved the

photocatalytic hydrogen evolution, Journal of Materials Science & Technology, 2022, 121, 28-39. https://doi.org/10.1016/j.jmst.2021.11.073

[7] Zhaobo Fan, Xin Guo, Zhiliang Jin, Xin Li, Youji Li, Bridging effect of S-C bond for boosting electron transfer over cubic hollow CoS/g-C3N4 heterojunction toward photocatalytic hydrogen production, Langmuir, 2022, 38(10), 3244-3256. https://doi.org/10.1021/acs.langmuir.1c03379

[8] Chuanbiao Bie, Bicheng Zhu, Linxi Wang, Huogen Yu, Chenhui Jiang, Tao Chen, Jiaguo Yu, "A bifunctional CdS/MoO2/MoS2 catalyst enhances photocatalytic H2 evolution and pyruvic acid synthesis." Angewandte Chemie International Edition, 2022, 61.44, e202212045.

[9] Xiaohong Li, Youji Li, Xin Guo, Zhiliang Jin,"Design and synthesis of ZnCo2O4/CdS for substantially improved photocatalytic hydrogen production." Frontiers of Chemical Science and Engineering, 2023,17.5, 606-616. https://doi.org/10.1007/s11705-022-2233-4

[10] Xuelian Yu, Xiaoqiang An, Alexey Shavel, Maria Ibáñez, Andreu Cabot, "The effect of the Ga content on the photocatalytic hydrogen evolution of CuIn1−x GaxS2 nanocrystals." Journal of Materials Chemistry A, 2014, 2.31, 12317-12322. https://doi.org/10.1039/C4TA01315H

[11] Wang Y, Peng J, Xu Y, *et al*. Facile fabrication of CdSe/CuInS2 microflowers with efficient photocatalytic hydrogen production activity. International Journal of Hydrogen Energy, 2022, 47(13), 8294-8302. https://doi.org/10.1016/j.ijhydene.2021.12.182

[12] Zhiliang Jin, Yanbing Li, Xuqiang Hao. Ni, Co-based selenide anchored g-C3N4 for boosting photocatalytic hydrogen evolution, Acta Physico-Chimica. Sinica., 2021, 37(10), 1912033.

[13] He Li, Ben Chong, Baorong Xu, Nathan Wells, Xiaoqing Yan, Guidong Yang, Nanoconfinement-induced conversion of water chemical adsorption properties in nanoporous photocatalysts to improve photocatalytic hydrogen evolution. ACS Catalysis, 2021, 11(22), 14076-14086. https://doi.org/10.1021/acscatal.1c03447

[14] Xuanpu Wang, Zhiliang Jin, Xin Li, "Monoclinic β-AgVO3 coupled with CdS formed a 1D/1D p-n heterojunction for efficient photocatalytic hydrogen evolution." Rare Metals, 2023, 42.5, 1494-1507. https://doi.org/10.1007/s12598-022-02183-y

[15] Yi Yang, Jinsong Wu, Bei Cheng, Liuyang Zhang, Ahmed Abdullah Al-Ghamdi, Swelm Wageh, Youji Li , Enhanced Photocatalytic H2-production Activity of CdS Nanoflower using Single Atom Pt and Graphene Quantum Dot as Dual Cocatalysts,Chinese Journal of Structural Chemistry , 2022, 41, 2206006-2206014.

[16] Kai Wang, Haiyan Xie, Youji Li, Guorong Wang, Zhiliang Jin, Anchoring highly-dispersed ZnCdS nanoparticles on NiCo prussian blue analogue-derived cubic-like NiCoP forms an S-scheme heterojunction for improved hydrogen evolution, Journal of Colloid and Interface Science, 2022, 628, 64-78. https://doi.org/10.1016/j.jcis.2022.08.001

[17] Yueqi Zhong, Jiangzhi Zi, Fan Wu, Zhao Li, Xue Luan, Fangfang Gao, Zichao Lian Defect-mediated electron transfer in Pt-CuInS2/CdS heterostructured nanocrystals for enhanced photocatalytic H2 evolution. ACS Applied Nano Materials, 2022, 5(6), 7704-7713. https://doi.org/10.1021/acsanm.2c00154

[18] Duc Quang Dao, Thi Kim Anh Nguyen, Sung Gu Kang, Eun Woo Shin, Engineering oxidation states of a platinum cocatalyst over chemically oxidized graphitic carbon nitride photocatalysts for photocatalytic hydrogen evolution. ACS Sustainable Chemistry & Engineering, 2021, 9(43), 14537-14549. https://doi.org/10.1021/acssuschemeng.1c05297

[19] Hui Liu, Lili Zhao, Jiayuan Yu, Guowei Xiong, Zhen Liu, Xiaoli Zhang, Benli Chu, Xiaoyan Liu, Hong Liu, Weijia Zhou. S doped Ta2O5 decorated CdS nanosphere via interfacial diffusion for enhanced and stable photocatalytic hydrogen production. Chemical Engineering Journal, 2022, 436, 131673. https://doi.org/10.1016/j.cej.2021.131673

[20] Zhenglong Xia, Rui Yu, Hong Yang , Bifu Luo , Yuanyong Huang , Di Li , Junyou Shi , Dongbo Xu Novel 2D Zn-porphyrin metal organic frameworks revived CdS for photocatalysis of hydrogen production. International Journal of Hydrogen Energy, 2022, 47(27), 13340-13350. https://doi.org/10.1016/j.ijhydene.2022.02.087

[21] Zhiliang Jin, Yanbing Li, Xuqiang Hao. Ni, Co-based selenide anchored g-C3N4 for boosting photocatalytic hydrogen evolution, Acta Physico-Chimica. Sinica., 2021, 37(10), 1912033.

[22] Zhiliang Jin, Hongying Li, Junke Li, Efficient photocatalytic hydrogen evolution over graphdiyne boosted with a cobalt sulfide formed S-scheme heterojunctions, Chinese Journal of Catalysis, 2022, 43(2), 303-315. https://doi.org/10.1016/S1872-2067(21)63818-4

[23] Yujie Ma, Xindong Wei, Kedeerya Aishanjiang, Yi Fu, Jiamei Le, Hailong Wu, Boosting the photocatalytic performance of Cu2O for hydrogen generation by Au nanostructures and rGO nanosheets. RSC advances, 2022, 12(48), 31415-31423. https://doi.org/10.1039/D2RA04132D

[24] Mengxue Yang, Youji Li, Zhiliang Jin, In situ XPS proved graphdiyne (CnH2n-2)-based CoFe LDH/CuI/GD double S-scheme heterojunction photocatalyst for hydrogen evolution, Separation and Purification Technology, 2023, 311, 123229. https://doi.org/10.1016/j.seppur.2023.123229

[25] Zhiliang Jin, Youlin Wu, Novel preparation strategy of graphdiyne (CnH2n-2): One-pot conjugation and S-Scheme heterojunctions formed with MoP characterized with in situ XPS for efficiently photocatalytic hydrogen evolution, Applied Catalysis B: Environmental, 2023, 327, 122461. https://doi.org/10.1016/j.apcatb.2023.122461

[26] Shanchi Liu, Kai Wang, Mengxue Yang, Zhiliang Jin. Rationally designed Mn0.2Cd0.8S@CoAl LDH S-scheme heterojunction for efficient photocatalytic hydrogen production, Acta Physico-Chimica. Sinica., 2022, 38(7), 2109023. https://doi.org/10.3866/PKU.WHXB202109023

[27] Yue Cao, Hongqian Gou, Pengfei Zhu, Zhiliang Jin, Ingenious design of CoAl-LDH p-n heterojunction based on CuI as holes receptor for photocatalytic hydrogen evolution, Chinese Journal of Structural Chemistry, 2022, 41, 2206079-2206085.

[28] Xiaoyan Zhang, Huijuan Huang, Yingguang Zhang, Dan Liu, Na Tong, Jinjin Lin, Lu Chen, Zizhong Zhang, Xuxu Wang. Phase transition of two-dimensional β-Ga2O3 nanosheets from ultrathin γ-Ga2O3 nanosheets and their photocatalytic hydrogen evolution activities. ACS omega, 2018, 3(10), 14469-14476. https://doi.org/10.1021/acsomega.8b01964

[29] Sheng Liu, Xueyi Guo, Weijia Wang, Ying Yang, Congtan Zhu, Chongyao Li, Weihuang, Qinghua Tian, Yong Liu, CdS-Cu1.81S heteronanorods with continuous sublattice for photocatalytic hydrogen production. Applied Catalysis B: Environmental, 2022, 303, 120909. https://doi.org/10.1016/j.apcatb.2021.120909

[30] Ruiqi Gao, Huan He, Junxian Bai, Lei Hao, Rongchen Shen, Peng Zhang, Youji Li, Xin Li, Pyrene-benzothiadiazole-based Polymer/CdS 2D/2D Organic/Inorganic Hybrid S-scheme Heterojunction for Efficient Photocatalytic H2 Evolution, Chinese Journal of Structural Chemistry, 2022, 41, 2206031-2206038.

[31] Zhiliang Jin, Application of graphdiyne in photocatalysis, Journal of The Chinese Ceramic Society, 2023, 51(1), 106-116.

[32] Na Su, Yang Bai, Zhonglian Shi, Jiale Li, Yixue Xu, Daoxiong Li, Baolu Li, Liqun Ye, Yi He, ReS2 Cocatalyst Improves the Hydrogen Production Performance of the CdS/ZnS Photocatalyst. ACS omega, 2023, 8(6), 6059-6066. https://doi.org/10.1021/acsomega.2c08110

[33] Haiming Gong, Youji Li, Hongying Li, Zhiliang Jin, 2D CeO2 and partial phosphated 2D Ni-based metal-organic framework formed S-scheme heterojunction for efficient photocatalytic hydrogen evolution, Langmuir, 2022, 38(6), 2117-2131. https://doi.org/10.1021/acs.langmuir.1c03198

[34] Junfeng Huang, Chenyang Li, Xiaoyun Hu, Jun Fan, Binran Zhao, Enzhou Liu, K2HPO4-Mediated Photocatalytic H2 Production over NiCoP/RP Heterojunction, Chinese Journal of Structural Chemistry, 2022, 41, 2206062-2206068.

[35] Mang Niu, Kunyan Sui, Xuesong Wu, Chunzhao Liu, Dapeng Cao. GaAs quantum dot/TiO2 heterojunction for visible-light photocatalytic hydrogen evolution: promotion of oxygen vacancy. Advanced Composites and Hybrid Materials, 2021, 1-11.

[36] Yonggang Lei, Xingwang Wu, Shuhui Li, Jianying Huang, Kim Hoong Ng, Yuekun Lai. Noble-metal-free metallic MoC combined with CdS for enhanced visible-light-driven photocatalytic hydrogen evolution. Journal of Cleaner Production, 2021, 322, 129018. https://doi.org/10.1016/j.jclepro.2021.129018

[37] Hongying Li, Haiming Gong, Zhiliang Jin. In2O3-modified Three-dimensional nanoflower MoSx form S-scheme heterojunction for efficient hydrogen production, Acta Physico-Chimica. Sinica., 2022, 38(12), 2201037.

[38] Guihao Zhong, Dingxin Liu, Biomorphic CdS/Cd Photocatalyst Derived from Butterfly Wing for Efficient Hydrogen Evolution Reaction. Advanced Materials Interfaces, 2022, 9(12), 2102423. https://doi.org/10.1002/admi.202102423

[39] Tian Wang, Zhiliang Jin, Graphdiyne (CnH2n-2) based CuI-GDY/ZnAl LDH double S-scheme heterojunction proved with in situ XPS for efficient photocatalytic hydrogen production, Journal of Materials Science & Technology, 2023, 155, 132-141. https://doi.org/10.1016/j.jmst.2023.03.002

[40] Youzhi Wang, Hongguang Jin, Yaopeng Li, Jing Fang, Chuansheng Chen, Ce-based organic framework enhanced the hydrogen evolution ability of ZnCdS photocatalyst. International Journal of Hydrogen Energy, 2022, 47(2), 962-970. https://doi.org/10.1016/j.ijhydene.2021.10.090

[41] Xuqiang Hao, Yifan Shao, Dingzhou Xiang, Zhiliang Jin, Photocatalytic overall water splitting hydrogen production over ZnCdS by spatially-separated WP and Co3O4 cocatalysts. Solar Energy Materials and Solar Cells, 2022, 248, 111970. https://doi.org/10.1016/j.solmat.2022.111970

[42] Xiuyuan Fan, Binfen Wang, Qianqian Heng, Wei Chen, Liqun Mao Facile in-situ synthesis of α-NiS/CdS pn junction with enhanced photocatalytic H2 production activity. International Journal of Hydrogen Energy, 2022, 47(76), 32531-32542. https://doi.org/10.1016/j.ijhydene.2022.07.265

[43] Xinjia Jia, Li Huang, Ruchao Gao, Perumal Devaraji, Wei Chen, Xiying Li, Liqun Mao, Improvement of photocatalytic hydrogen generation of leaves-like CdS microcrystals with a surface decorated by dealloyed Pt-Cox nanoparticles. Solar Energy, 2020, 206, 8-17. https://doi.org/10.1016/j.solener.2020.05.073

Received on 15-04-2023 Accepted on 08-06-2023 Published on 21-06-2023

DOI: https://doi.org/10.31875/2410-2199.2023.10.03